# Digitization of Holographic Interferograms for Deflection Measurement

*J. A. Gilbert*

Associate Professor of Engineering Mechanics
University of Wisconsin-Milwaukee
Milwaukee, Wisconsin 53201

*T. D. Dudderar*

AT&T Bell Laboratories
600 Mountain Avenue
Murray Hill, New Jersey 07974

*D. R. Matthys*

Associate Professor of Physics
Marquette University
Milwaukee, Wisconsin 53233

*J. H. Chern*

Research Assistant
University of Wisconsin-Milwaukee
Milwaukee, Wisconsin 53201

*ABSTRACT*

The underlying principles of a carrier fringe technique necessary for automated holo-interferometric data acquisition and analysis are discussed, and a practical method for monitoring two-dimensional real-time deformation is demonstrated. This method uses a "real-time" holocamera to record reference holograms, real-time immediate processing photography to capture background intensity, carrier fringe and deformation/carrier fringe patterns, a high resolution vidicon camera/electronic package to digitize the resulting two-dimensional intensity distributions and a computer for fast data reduction and interpretation. Such a system significantly reduces the amount of effort and time normally required to extract the desired information from holo-interferometric fringe fields by conventional means. Furthermore, the proposed approach minimizes subjective evaluation of fringe data by the investigator and eliminates the ambiguity associated with the displacement equations governing holographic interferometry. The present work is limited to measurement of static deflections but the general approach can be easily extended to more complex dynamic displacements.

## Introduction

Holographic techniques have been of interest to the stress analyst for many years, but so far industry has proven reluctant to employ holographic interferometry to any significant extent. This has been largely due to the many stringent requirements that are inherent to both holography and interferometry. These include the necessity of isolating all optical components from vibration, the long turnaround time required for processing holograms, the need for highly trained technicians to set up equipment, and the great deal of effort and energy required to interpret the results. Recent technological advances, however, have helped to ease these constraints. For example, fiber optic components can now be used as environmentally less sensitive elements to manipulate the object illumination and/or reference beams to facilitate set-up in areas of structures which may be significantly removed from the recording site [1]. Commercially available holocameras (such as the Newport HC310 Holocamera, or the Laser Technology Holomatic 6000) make it possible in many cases to record and view real-time deformation-related holo-interferograms within seconds. However, it still requires a great deal of time, effort and sophistication to reliably interpret these fringe patterns and determine the full field of deformation in even the simplest of cases. Fortunately, recent developments in image digitization and computer based numerical processing techniques raise the potential for automating much, and possibly all, of the fringe analysis procedure for even the most complicated problems.

There have been many attempts to digitally process holo-interferometric fringe patterns, but the majority of these efforts have involved the characterization of linear fringe distributions produced by simple translations or nearly homogeneous deformations [2-6]. In most cases, computer analysis of more complicated holo-interferometric fringe patterns has been limited to qualitative analysis [7] or has required a substantial amount of direct interaction on the part of the operator [8]. Unfortunately, most structural defects and stress concentrations are accompanied by highly non-homogeneous strains which produce very complicated holo-interferometric patterns from which detailed quantitative results must be obtained. Figure 1, for example, shows reconstructions of doubly exposed holograms recorded to establish needed mechanical characteristics of VLSI (very large scale integration) packages [9].

The interpretation of a more regular fringe pattern, though tedious, can be relatively straightforward provided that the investigator knows the geometry of the recording system and has some knowledge of the expected behavior of the surface. But even a trained observer completely familiar with the optical configuration used to generate the patterns shown in Figure 1 would not be able to unambiguously interpret such complex fringe patterns based on visual inspection alone. Even if digitized and fed into a computer, such patterns would be very difficult to

analyze correctly. In such cases the actual surface deflections are simply too complex. Has the surface moved towards or away from the observer? What if a saddle point appears in the field? Where are deflections monotonically increasing or decreasing? These are fundamental questions that must be addressed in order to develop a satisfactory automated computer-based approach to stress analysis involving complex holographic interferograms.

Katzir et al [10] demonstrated that these questions may be answered by introducing an appropriate carrier fringe pattern and detecting the intensity distribution by mechanically scanning with a linear diode array. The present study demonstrates a full field system that uses both fiber optics and a vidicon camera/digitizer to facilitate acquisition of two-dimensional information from carrier fringe fields which can be rapidly and efficiently interpreted by a suitably programmed computer.

**Holographic Displacement Analysis**

The fringes in a holographic interferogram taken from a diffuse surface are related to the wavelength, the geometry of illumination and observation, and the displacement of the surface by the simple vector expression,

$$\underline{k} \cdot \underline{d} = n_d \lambda \tag{1}$$

where $n_d$ is the fringe order number, $\lambda$ is the wavelength of coherent light used to record and reconstruct the hologram, $\underline{k}$ is the sensitivity vector $(\underline{i}_2 - \underline{i}_1)$ where $\underline{i}_1$ and $\underline{i}_2$ are unit vectors in the illumination and observation directions respectively, and $\underline{d}$ is the mechanical displacement at the point of observation on the surface of the sample.

Quantitative analysis may be considerably simplified by positioning optical components in the recording system to favor the measurement of a preferred displacement component. For example, Figure 2 illustrates a simplified version of a holographic/fiber optic set-up previously investigated by two of the authors for making real-time measurements [11] on a planar subject. Here single mode optical fibers (SMFs) are used to illuminate the object and as a source for the reference beam. The hologram itself is recorded on a thermoplastic device in an experimental layout in which the normal to the object under study is intentionally positioned along the bisector of the angle, $2\beta$, between the illumination and observation vectors. In this case, the interferometer senses only the out-of-plane displacement (or deflection), $W$, and Equation 1 reduces to

$$2\, W \cos \beta = n_d \lambda \tag{2}$$

**Digitization**

Figure 3 shows a schematic of the photoelectronic-numerical processing system designed for image digitization, recording and computer analysis. The holographic fringe pattern is imaged into a high resolution vidicon camera. Digitized data taken from the image is stored on an LSI 11/23 microprocessor as a 1024 × 1024 array with each element (pixel) containing 8 bits of information (0-255 grey levels). Images can be previewed in the LSI 11/23 before being transferred to a VAX for further processing, and the results can be displayed using a commercial graphics package.

The relevant information about the surface displacement, $W$, is derived from the holo-interferogram by determining the locations of the fringes which represent the phase distribution of the interference. In some cases raw data is sufficient to crudely estimate fringe maxima. However, even in the best images this information is not always sufficient to assign unique fringe orders in the digitized pattern. Figure 4, for example, shows a reconstruction of a fringe pattern recorded with the set-up shown in Figure 2, in which fringes represent deflections caused by a concentrated load applied to the center of a circular† disk clamped around its boundary. A plot of the digitized intensity along the vertical center line labeled AB is shown at the left of Figure 4. Fringes corresponding to peaks in the plot labeled 2-8 can be easily recognized and located by the computer, especially when filtering and smoothing techniques are applied. However, this information by itself is insufficient to determine unique fringe orders, even for such a simple test, since the computer has no way to establish that, for example, peaks 3 and 7 lie on the *same fringe*. The fringe count could be enumerated using sophisticated software routines to track fringe loci throughout the entire image, but such an approach would be time consuming and extremely difficult to accomplish in the presence of normal speckle noise. Moreover, if circumstances were such that fringes of the same order were not all interconnected within the viewable image, as is often the case, even such sophisticated numerical image analysis routines would probably fail. These problems do not occur in cases where the phase variations are monotonic along a data line, since in such cases the same fringe order would never be scanned twice. (Here the term "data line" is used to describe the line AB and all similar lines along which the fringe distribution must be determined and analyzed in order to evaluate the deformation field.) Unfortunately, however, a second problem prohibits completely rigorous analysis even in cases where the phase distribution is monotonic. This is so because, even though Equations 1 and 2 are sufficient to analyze displacements due to changes in phase, both are somewhat ambiguous, since positive and negative phase changes (distributions) can both produce the same holo-interferometric fringe patterns. Equation 2, for example, describes the pattern shown in Figure 4, but it is impossible to determine from visual inspection of that pattern whether the surface has moved *towards* or *away from* the observer.

This problem has been addressed for the digitization and computer analysis of moire fringe patterns [12], and can be solved in the present study by introducing a known high frequency linear carrier into the holo-interferometric fringe pattern while observing the direction of fringe shift [13]. More importantly, the carrier can be adjusted to force the phase to become monotonic over each line of the data in the stored image [14], thereby facilitating unambiguous, efficient computation. Of course, the carrier fringes should be aligned normal to the lines of data along which the fringe distribution is to be evaluated [10].

**Further Holographic Analysis**

Linear holographic carrier patterns can be generated by moving either the model, the illumination, the reference beam, or the hologram itself [15]. Any of these produces a phase shift, $\delta$, governed by:

$$\delta = n_c \lambda \tag{3}$$

A displacement of the object causes additional phase changes to be superimposed on those of the carrier as follows:

$$\delta + \underline{k} \cdot \underline{d} = (n_d + n_c)\lambda = n\lambda \tag{4}$$

Equation 1 results when Equation 3 is subtracted from Equation 4. This can actually be accomplished by optical means if the holo-interferograms corresponding to Equations 3 and 4 are photographically recorded and physically superimposed to produce a moire. Such optical processing requires a high density carrier and usually involves filtering to enhance fringe contrast.

On the other hand, if such a superimposed carrier and displacement fringe pattern is digitized, it can be reliably interpreted and numerically analyzed by a suitably programed computer, using relatively low (but more readily resolvable) carrier frequencies that would not suffice for optical processing. Computer processing has the added advantage that numerical results can be stored for graphical display and/or further analysis.

**Experiments**

Experiments to demonstrate the proposed carrier fringe technique were conducted on a 1.6mm thick glass disk of 88mm diameter. This disk was bonded around its circumference (leaving a free diameter of 80mm) to a stiff ring mounted in a two axis gimballed holder with a

† This reconstruction was photographed directly from a high resolution TV monitor which had different gains in the horizontal and vertical directions; consequently, the circular image appears slightly ellipitical.

central loading micrometer. The model was positioned in the configuration shown in Figure 2 with the normal to the surface aligned with the angle bisector of the illumination/observation directions so that the resulting fringes are the loci of constant normal or out-of-plane displacement (deflection) with a fringe-to-fringe sensitivity of 0.320$\mu$m at a wavelength of 0.633$\mu$m. Figure 4 shows the holo-interferometric fringe field recorded after the center of the disk was displaced 1.28$\mu$m outward or "towards the viewer," while Figures 5a and 5b show the modified fringe patterns as a linear carrier was added to the fringe field by progressively tilting the disk around a horizontal axis through 0.0014 and 0.0062 degrees, respectively. The bottom of the disk moved outward in both cases. Therefore the carrier fringe order must *increase* from the top to the bottom of the subject. This "polarity" would be reversed if the carrier fringes were generated by reverse tilt in which the top of the subject is moved outward, but the linear fringe pattern would *look* just the same.

Figure 6 shows smoothed plots of the fringe order numbers as distributed along the line AB (see Figure 4) for Figures 4, 5a and 5b. The plot of the deformation (the curve for Figure 4) is not monotonic across AB but as the carrier is introduced, the circular fringes in the original pattern tend to straighten out and the combined deformation/carrier plots become monotonically increasing over this line. Figure 5a, for example, shows only a hint of the original circular pattern, and the corresponding plot shown in Figure 6 is nearly monotonic (the ideal condition for digitization). The fringe pattern in 5b is monotonic and, when digitized, the fringes can be reliably located and enumerated along any appropriate line by the computer. In the next step, the phase distribution corresponding to the carrier must be removed in order to uniquely determine both the magnitude and sign of the imposed deformation. This might be accomplished by first analyzing the deformation/carrier pattern and then numerically subtracting the carrier. Unfortunately, however, the digital image of the interferogram always contains noise. The coherent illumination coupled with surface irregularities causes optical noise (variations in average intensity and contrast over the field) ranging from the low frequency variation in intensity created by a Gaussian illumination to the high frequency modulations caused by objective and/or subjective speckling. These, together with detection errors (variations in leakage current and sensitivity, amplification errors and noise, quantization error, etc.) seriously hamper the task of determining fringe maxima. Fortunately, the deleterious effects of many of these errors can be minimized by using the method of image intensity subtraction [6].

This method can be demonstrated optically by superimposing (by double exposure photography) reconstructions of a relatively high frequency carrier pattern (generated by tilting the disk through 0.0119 degrees, as was done for Figure 7a) with the corresponding deformation/carrier pattern (for a center deflection equal to 1.60$\mu$m, as was done for Figure 7b). The resulting moire of circular fringes, characteristic of a centrally loaded disk, is shown in Figure 8 along with a comparable doubly exposed hologram. The same result could be obtained numerically by simply subtracting the intensities stored in the file of the digitized carrier pattern from those contained in the file of the digitized deformation/carrier pattern. The resulting image intensity subtraction eliminates many errors due to noise, but the process alone cannot produce enough reliable information to accurately locate fringes and specify the sign of the displacement. This requires separate "normalized" (corrected for "background") files for both the carrier and deformation/carrier patterns.

To obtain this required information, a hologram of the unloaded disk was recorded and the object illumination and reconstructing reference beams adjusted to yield reasonably balanced object wavefronts of appropriate intensity. These two "background" images were then combined in a single reference image by successively recording one and then the other in a doubly exposed photograph. This photograph was then digitized to produce a file containing the background intensity distribution with no interference fringes. Next a holo-interferometric carrier fringe pattern was generated in real-time and recorded. Finally the model was loaded and a real-time deformation/carrier fringe pattern was also recorded. In order to provide temporal smoothing or frame averaging usually required for data acquisition in a real-time system, each pattern was initially photographed on high speed Polaroid film (3000 ASA) and then digitized. This technique can be applied directly to highly dynamic events using high speed photography. The background intensity distribution was then subtracted on a pointwise (pixel) basis from both the carrier and the deformation/carrier files to produce the "normalized" files required for subsequent analysis.

In the next step, fringe orders were assigned to the normalized carrier pattern over each data line, in every case observing the correct polarity.† Assigning any set of monotonically increasing orders (of the same polarity as the carrier) to the fringes in the normalized deformation/carrier pattern will determine the surface contours of correct sign to within an additive constant, regardless of the complexity of the deformation field. If, as is often the case, a zero order (no deformation) fringe is present, the precise carrier fringe orders can be assigned and an exact solution can always be obtained. In the present case we know both that (1) the outer edge of the disk is clamped, so that the boundary deformations must be zero, and (2) that the horizontal center line of the disk (axis of carrier rotation) is a zero order carrier fringe. Consequently, absolute deflections can be calculated along each line by enumerating the fringe orders from minus numbers at the top to plus numbers at the bottom, (as was done with the line of fringe data taken from Figure 5b and plotted in Figure 6), and subtracting the fringe orders in the normalized carrier pattern from those in the normalized deformation/carrier pattern pixel by pixel, thus generating a map of the surface contours. Figure 9 shows the successful result of applying this approach to the carrier and deformation/carrier patterns shown in Figures 7a and 7b, respectively.

Finally, if as sometimes happens, there is no fixed boundary or fringe of known order within the observable/recordable fringe field, and if knowing the entire deformation field to within a constant is not sufficient,† then even the most complicated, otherwise ambiguous case can still be evaluated reliably and accurately by simply following the shift of any suitable carrier fringe during loading in order to establish an appropriate reference.

**Conclusions**

A computer based vidicon camera system has been demonstrated with the capacity to digitize, store and accurately analyze high speed photographs of real-time holo-interferometric, fringe fields. Key to this approach is the use of a superimposed carrier fringe pattern to remove intrinsic ambiguities, and the recording of reference or "background" intensity distributions. While the present work was concerned with the evaluation of a simple field of out-of-plane static deformation on a two-dimensional planar surface, it confirms, in principal, a fundamental approach to the eventual development of automated holo-interferometric systems for the efficient, quantitative evaluation of complex, multidimensional, dynamic displacement fields.

Future work will focus on the application of computer-oriented carrier fringe techniques and digital image analysis to the study of more complex general displacement fields, and applications to remote optical metrology through the use of fiber optics. This will include exploration of the potential for using automated fiber optic holo-interferometric systems as tools for on-line data acquisition and analysis in military, industrial, medical and educational environments.

**Acknowledgements**

This work was supported by the U. S. Army Research Office under Contract Nos. DAAG 29-84-K-0183 and DAAG 29-84-G-0045, the Graduate School at the University of Wisconsin-Milwaukee, and by AT&T Bell Laboratories.

† In the present example the chosen direction of tilt (out at the bottom, in at the top) requires that the fringe order increase from top to bottom.

† In strain field analysis knowledge of this constant is not required.

## REFERENCES


[1] Gilbert, J. A., Dudderar, T. D., Applications of fiber optics to coherent metrology for the study of material deformations and structural mechanics, Army Symposium on Solid Mechanics, Newport, Rhode Island, October 1-3, 1984, p. 63-92.

[2] Katzir, Y., Glaser, I., Friesem, A. A., Sharon, B., On-line acquisition and analysis for holographic nondestructive evaluation, Optical Engineering, 21, 6 (1982), p. 1016-1021.

[3] Hot, J. P., Durou, C., System for the automatic analysis of interferograms obtained by holographic interferometry, SPIE 2nd. European Congress on Optics Applied to Metrology, 210 (1979), p. 144-151.

[4] Lamy, F., Liegeois, C., Meyrueis, P., Automatic computer analysis of double exposure hologram in industrial nondestructive control, Proceedings of the Soc. of Photo-optical Instrumentation Engineers, 353 (1983), p. 82-89.

[5] Kreis, T. M., Kreitlow, H., Digital processing of holographic interference patterns, OSA/SESA Topical Meeting on Holography Interferometry and Speckle Metrology, Cape Code, Mass. (1980), Paper No. TuB2.

[6] Lanzl, F., Schluter M., Microprocessor-controlled hologram analysis, IEEE 5th. International Computing Conference, London (1978), p. 159-162.

[7] Tichenor, D., A., Madsen, V. P., Computer analysis of holographic interferograms for nondestructive testing, SPIE Image Understanding Systems & Industrial Applications, 155 (1978), p. 222-227.

[8] Leif, E., Majlof, L., Evaluation of 3-D displacements by holography and computer, OSA/SESA Topical Meeting on Holography Interferometry and Speckle Metrology, Cape Cod, Mass. (1980), Paper No. TuB3.

[9] Dudderar, T. D., Hall, P. M., Gilbert, J. A., Holo-interferometric studies of the thermal deformations in microelectronic modules, Proceedings of the 1985 Society for Experimental Mechanics Spring Conference on Experimental Mechanics, Las Vegas, Nevada (1985) available mid 1985.

[10] Katzir, Y., Friesem, A. A., Glaser, I., Sharon, B., Holographic nondestructive evaluation with on line acquisition and processing, *Industrial and Commercial Applications of Holography*, Milton Chang, Editor, Proc., SPIE 353 (1982), p. 74-81.

[11] Dudderar, T. D., Gilbert, J. A., Real-time holographic interferometry through fiber optics, J. Phys. E: Sci. Instrum., 18 (1985), p. 39-43.

[12] Milly, T. M., Hunter, A., Application of computerized data acquisition and data processing to the surface contouring of large structures, Proceedings of the SESA 5th Int. Congress on Exp. Mech., Montreal, Canada (1984), p. 795-799.

[13] Sciammarella, C. A., Ahmadshahi, M., A computer based method for fringe pattern analysis, Proceedings of the 1984 SEM Fall Conference, Milwaukee, Wisconsin (1984), p. 61-69.

[14] Plotkowski, P. D., Hung, Y. Y., Hovanesian, J. D., A fringe carrier technique for the unambiguous determination of holographically recorded displacements, Proceedings of the SPIE Technical Symposium on Optical & Electro-Optical Engineering, Los Angeles, California (1985), available mid-1985.

[15] Beranek, W. J., Bruinsma, A. J. A., A geometrical approach to holographic interferometry, Experimental Mechanics, 20, 9 (1980), p. 289-300.


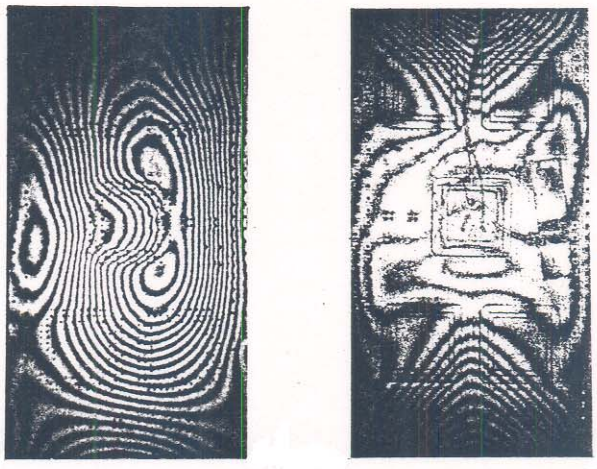


Figure 1 Thermally Induced Deflection Patterns on VLSI Modules

a. On the Back of a Module with a Single Surface-Mounted Microelectronic Component

b. On the Front of a Module with Five Surface-Mounted Microelectronic Modules

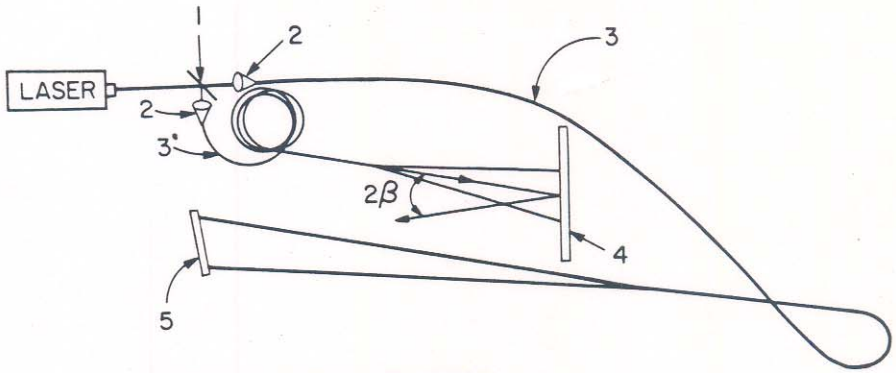


1 - VARIABLE BEAM SPLITTER
2 - FIBER LAUNCH OPTICS
3 - SINGLE MODE OPTICAL FIBER
4 - MODEL
5 - HOLOGRAM PLATE

Figure 2 Real-Time Holographic/Fiber Optic Set-Up

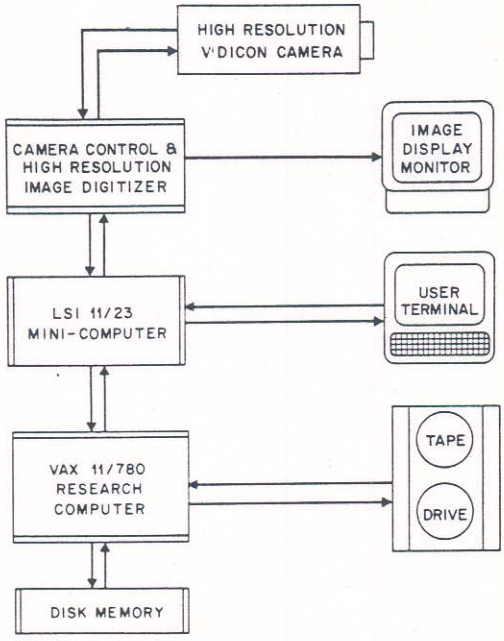


Figure 3 Photoelectronic/Numerical Recording and Analysis System

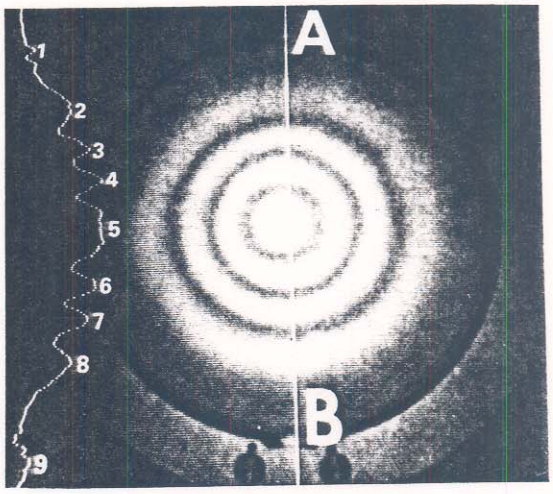


Figure 4 Centrally loaded Disk Showing an Intensity Plot along the Vertical Center Line (AB)

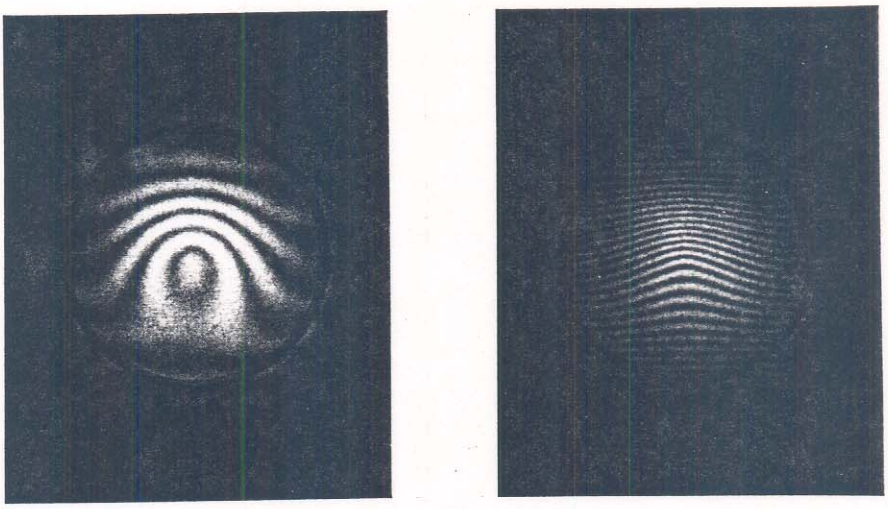


Figure 5 Holo-interferograms of the Disk

a. 1.28$\mu$m Center Deflection at 0.0014 Deg. Tilt

b. 1.28$\mu$m Center Deflection at 0.0062 Deg. Tilt

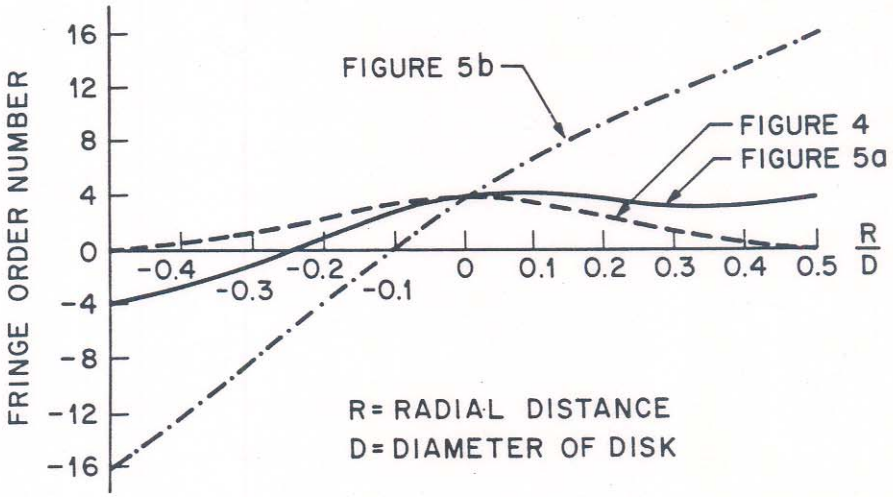


Figure 6 Plots of Fringe Data along Vertical Center Line (AB) from Figures 4, 5a and 5b

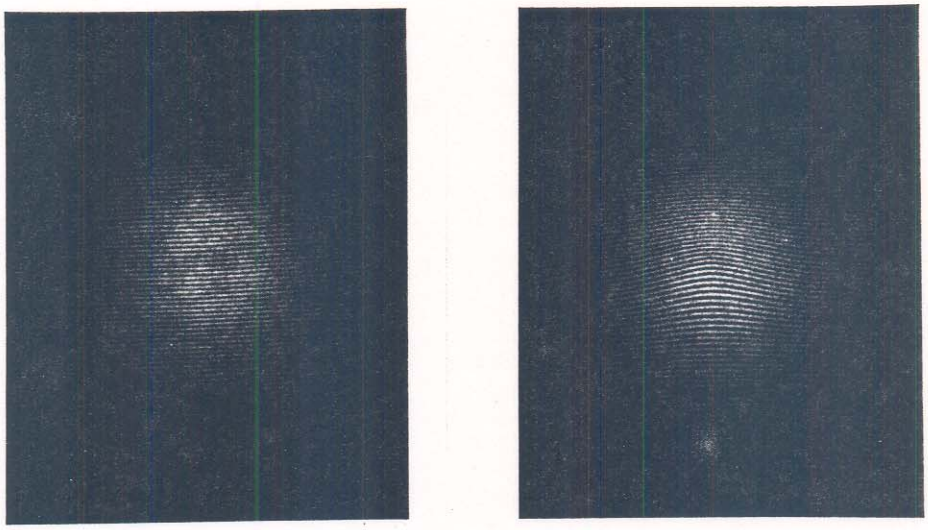

(a) (b)

Figure 7 Carrier and Deformation/Carrier Patterns with

a. Zero Center Deflection at 0.0119 Deg. Tilt

b. 1.60$\mu$m Center Deflection at 0.0119 Deg. Tilt

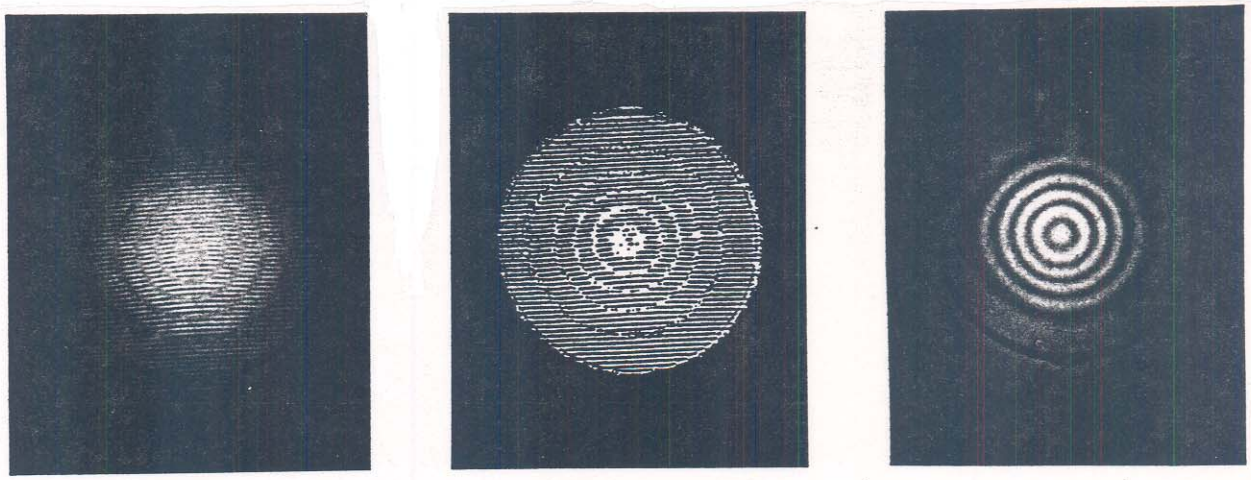

(a) (b) (c)

Figure 8 Holo-interferograms of the disk with a 1.60$\mu$m Center Deflection

a. From a Moire of Patterns Shown in 7a and 7b As Recorded in a Double Exposed Half Tone Photograph

b. As seen in a Very High Contrast Reproduction of the above and

c. From a Double Exposed Hologram.

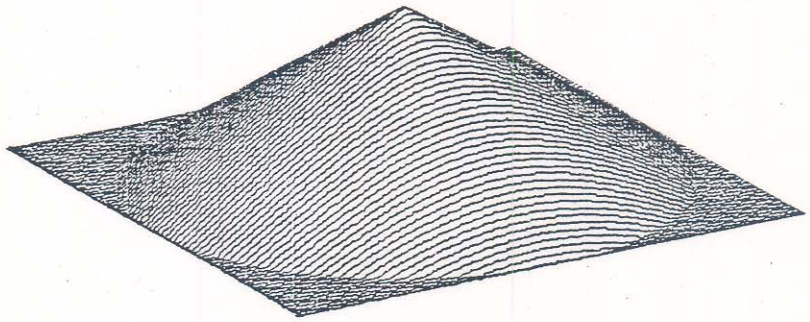

Figure 9 Isometric Plot of the Measured Deformation of the Disk